Earth Planet. Sci. Lett. 626 (2024) 118558

Contents lists available at ScienceDirect

Earth and Planetary Science Letters

journal homepage: www.elsevier.com/locate/epsl

# Olivine-catalyzed glycolaldehyde and sugar synthesis under aqueous conditions: Application to prebiotic chemistry

Vassilissa Vinogradoff [a,*], Vanessa Leyva [b], Eric Mates-Torres [c], Raphael Pepino [b], Grégoire Danger [a], Albert Rimola [c], Lauryane Cazals [a], Coline Serra [a], Robert Pascal [a], Cornelia Meinert [b,*]

[a] CNRS, Institut Origines, Université Aix-Marseille, PIIM UMR CNRS 7345, Marseille, France
[b] CNRS, Université Côte d'Azur, ICN UMR CNRS 7272, Nice, France
[c] Departament de Química, Universitat Autònoma de Barcelona, Bellaterra, Catalonia 08193, Spain

ARTICLE INFO

Editor: H. Bao

*Keywords:*
Olivine catalysis
Formose reaction
Sugars
Phyllosilicates
Prebiotic chemistry
Aqueous alteration

ABSTRACT

The presence of minerals in the prebiotic environment likely shaped the evolution of organic matter, thereby contributing to the emergence of prebiotic systems. Records of such systems are lacking and the interactions between abiotic organic matter and primary minerals remain poorly understood. Here, we demonstrate the ability of olivine silicates, in simulated early Earth or planetary aqueous environments, to catalyse glycolaldehyde formation from only formaldehyde, and help producing sugars that are essential components for life, through the formose reaction. By combining comprehensive gas chromatography analyses on experimental samples with quantum chemical simulations, we provide a mechanism for an olivine-catalyzed glycolaldehyde formation. Our findings suggest that olivine plays a triple role in the formose chemical network: maintaining an alkaline pH, enabling the initiation step towards the formation of glycoladehyde (which is typically the most challenging step) and promoting the autocatalytic cycle. These results open-up new scenarios on the impact of primary minerals on the evolution of chemical pathways in aqueous environments that were probably essential for the emergence of the first biomolecules.

## 1. Introduction

Sugars are important molecules of great biological significance for Earth life. Found in cometary-like analogs (Meinert et al., 2016) and carbonaceous meteorites (Cooper et al., 2001; Furukawa et al., 2019), sugars may have played a pivotal role in the emergence of prebiotic systems on Earth by being delivered through extraterrestrial materials. However, sugars are unstable in aqueous environments (Larralde et al., 1995), and any contributions to the origin of life would require a continuous source of these compounds. In dedicated aqueous environments, the formation of sugars might have happened on early Earth or other planetary surfaces. A plausible route for their formation may have been the formose reaction that converts formaldehyde into more complex sugars (Fig. 1) (Breslow, 1959; Butlerov, 1861). Formaldehyde is thought to have been abundant on early Earth and has been recognized for its prebiotic potential (Cleaves, 2008). However, the formose reaction itself is not a straightforward or simple chemical reaction network and requires certain conditions to proceed efficiently. For example, several parameters such as pH, temperature, or formaldehyde concentration can either inhibit or promote sugar formation (see reviews by Delidovich et al., 2014; Kopetzki and Antonietti, 2011; Mizuno and Weiss, 1974). The presence of a catalyst, usually a mineral, is a key condition to sustain the autocatalytic cycle for the aldol and retro-aldol reactions to form carbohydrates (Cairns-Smith et al., 1972; Delidovich et al., 2014; Gabel and Ponnamperuma, 1967; Lambert et al., 2010). In addition to the catalyst, an initiator is also required for the self-condensation of formaldehyde towards the first important and simplest sugar of the autocatalytic cycle, glycolaldehyde (Kopetzki and Antonietti, 2011). In the absence of glycolaldehyde, only the Cannizzaro reaction, which results in the disproportionation of formaldehyde into methanol and formic acid, occurs in aqueous formaldehyde solutions (Schwartz and de Graaf, 1993). Moreover, the direct dimerization of two formaldehyde molecules—two electrophiles—is very slow in water and is deemed chemically unfeasible in the absence of a catalyst since

* Corresponding authors.
*E-mail addresses:* vassilissa.vinogradoff@univ-amu.fr (V. Vinogradoff), cornelia.meinert@univ-cotedazur.fr (C. Meinert).

https://doi.org/10.1016/j.epsl.2023.118558
Received 2 October 2023; Received in revised form 20 December 2023; Accepted 22 December 2023
Available online 29 December 2023

deprotonation and polarity inversion (*umpolung*) is necessary. This slow process has long been thought to make the formose reaction unlikely to contribute to prebiotic systems. However, UV irradiated formaldehyde solutions do produce highly branched sugars (Shigemasa et al., 1977) likely via hydroxymethylene, as shown from gas-phase reactions (Eckhardt et al., 2018), making the activation of the formose reaction possible in water (Ritson and Sutherland, 2012). Over the years, many other agents including acids, salts, hydroxides, and minerals have been tested to better constrain the mechanism of the formose reaction and its limitations in solution (Kopetzki and Antonietti, 2011). Glycolaldehyde itself was found to be the most efficient initiator, while calcium hydroxide ($Ca(OH)_2$), with its divalent cation that coordinates the enediol forms of sugars, proved to be the optimal catalyst (Delidovich et al., 2014; Kopetzki and Antonietti, 2011). Another approach involves a mechanochemical sugar synthesis mediated by various minerals in water-free, prebiotic geochemical settings, which has been demonstrated to greatly minimize side and decomposition reactions (Haas et al., 2020). However, none of these studies could accomplish an effective formose reaction using solely formaldehyde in the starting solution.

In this study, we aimed to explore the formose reaction under conditions that could have been similar to various aqueous environments on early Earth or other planetary surfaces such as Mars. We performed the reaction in mid-temperature aqueous conditions (80 °C) with an ubiquitous silicate mineral on early Earth formed in volcanic settings, i.e. olivine (Miyazaki and Korenaga, 2022; Russell and Ponce, 2020). Our approach allowed us to better understand how minerals can interact and drive abiotic chemical reactions of prebiotic significance under realistic geological settings, an area of research that is still in its early stages. Olivine was found to effectively activate formaldehyde to form the initial reactive intermediate, the glycolaldehyde monomer, enabling the catalysis of the rest of the formose reaction cascade. Our detailed analytical monitoring revealed the formation of various sugar and sugar-related molecules exhibiting comparable molecular diversity to the conventional calcium hydroxide catalyst. Through computational surface modeling of olivine and its interaction with formaldehyde, we have gained mechanistic insights of the molecular processes involved in activating formaldehyde and the subsequent formation of glycolaldehyde, this way corroborating our experimental results. Transposing a plausible sugar reaction network to conditions relevant to early Earth, with the majority of the key components and actors involved in these reactions, is key to elucidate the chemical pathways that potentially played a role in the emergence of self-organized chemical networks at the origin of life.

## 2. Experimental

### 2.1. Material and methods

#### 2.1.1. Hydrothermal alteration experiments

The Mg-rich olivine was obtained from San Carlos, Arizona (namely peridot), and has an approximate composition of $Mg_{1.8–1.9}Fe_{0.2–0.1}SiO_4$. The cm to mm-sized grains were washed several times with different solvents including water (Milli-Q® grade, Direct, Merck, 18.2 MΩ $cm^{-1}$), dichloromethane (DCM, Sigma Aldrich-HPLC grade 99.8 %) and methanol (Sigma-Aldrich HPLC grade 99.9 %) to remove external organic contamination before grinding. The grains were then ground to micrometer size (<10 μm) to maximize their surface reactivity. The light-grey powder was rewashed with DCM and methanol to further minimize organic contamination, and then dried in an oven at 60 °C for 48 h. Formaldehyde (in the form of polyoxymethylene, POM-grade 95–100 %), glycolaldehyde (under the form of dimer-grade 100 %), and calcium hydroxide (grade 99.9 %) were purchased in the highest possible purity from Sigma-Aldrich. The use of powdered POM was preferred over aqueous solutions of paraformaldehyde to deliver formaldehyde, primarily to minimize the potential presence of carbohydrate contaminants. Milli-Q® water used for the experiments was degassed with nitrogen prior to utilization. The solutions were prepared in an anoxic chamber under an argon atmosphere (>99.999 %, Air liquid ALPHAGAZ 1). Formaldehyde (F) concentrations were set at 10 g $L^{-1}$, olivine (O) at 100 g $L^{-1}$, glycolaldehyde (G) at 1 g $L^{-1}$, and calcium hydroxide (α) at 1.5 g $L^{-1}$. The total volume of the solutions was 1 mL, yielding a water-to-rock ratio of 10. Solutions were all prepared in a glove box, loaded into closed quartz cells, inserted into PTFE reactors, and made airtight in hydrothermal reactors (Toption) under an argon atmosphere. The reactors were then removed from the glove box and placed in an oven at 80 °C for 2, 7 or 45 days (one solution for each duration). We tested different combinations of reactants, O, F, FO, FG, FGO, Fα, FGα

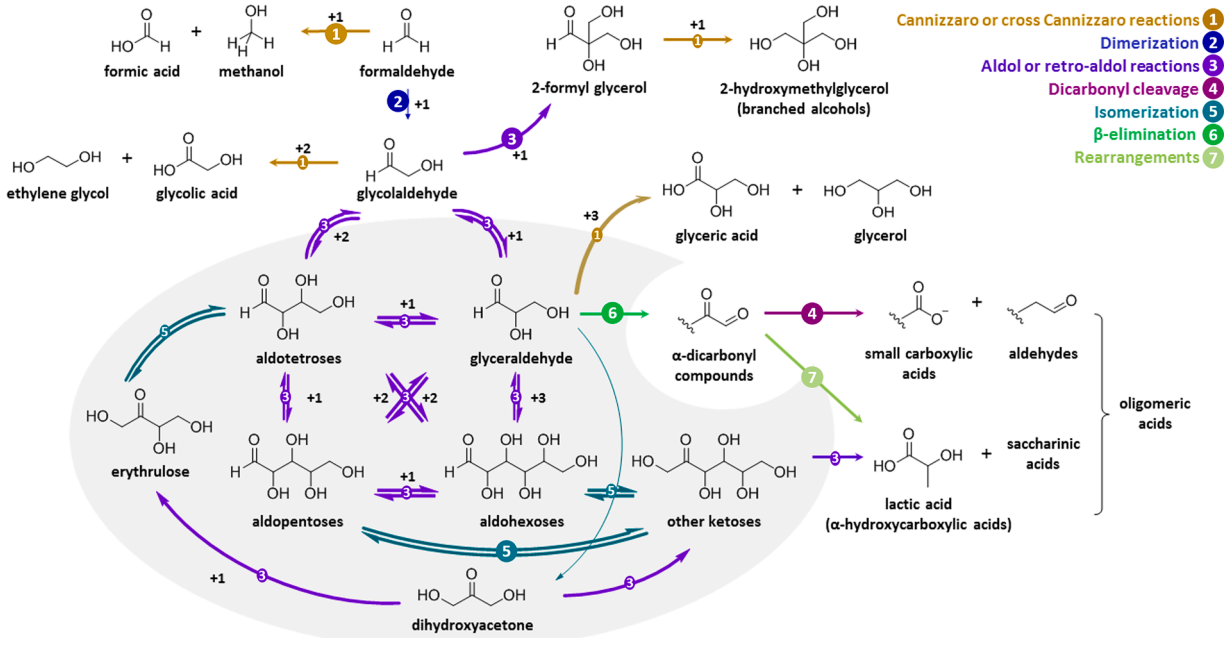


**Fig. 1.** Overview of the formose autocatalytic reaction network. The production of monosaccharides (grey area) and competing reaction pathways, such as the Cannizzaro reaction that generates sugar acids and sugar alcohols, are illustrated.

**Table 1**
Overview of samples studied in this work in anoxic conditions under hydrothermal alteration at 80 °C for different durations[a].

| sample | Composition | Day 2 | Day 7 | Day 45 |
|---|---|---|---|---|
| F | formaldehyde | F2 | – | F45 |
| FG | formaldehyde + glycolaldehyde | FG2 (pH = 4–5) | FG7 (pH = 3–4) | FG45 (pH = 4) |
| O | olivine | O2 | O7 | – |
| FO | formaldehyde + olivine | FO2 (pH = 6–7) | FO7 (pH = 6–7) | FO45 (pH = 6) |
| FGO | formaldehyde + glycolaldehyde + olivine | FGO2 (pH = 7) | FGO7 (pH = 6–7) | FGO45 (pH = 7) |
| Fα | formaldehyde + $Ca(OH)_2$ | Fα2 (pH = 5–6) | Fα7 (pH = 5) | – |
| FGα | formaldehyde + glycolaldehyde + $Ca(OH)_2$ | FGα2 (pH = 6–7) | FGα7 (pH = 5) | – |

[a] The pH was measured at the end of each experiment using pH test strips.

(Table 1). After the completion of the experiments, samples with minerals were centrifuged to separate the solids from the liquids (15 min at 13,000 rpm). The supernatants were recovered for the identification and quantification of sugar and sugar-related compounds by multidimensional gas chromatography. The solid residues were dried in an oven and stored for further analyses.

### 2.2. Gas chromatographic analysis

From each sample, 20 µL were transferred into a Reactivial® and dried under a gentle stream of nitrogen. To each vial, 50 µL of a 10 mg $mL^{-1}$ methylboronic acid (MBA) solution in pyridine were added, stirred for 10 s, and heated for 30 min at 60 °C. The samples were then allowed to cool down to room temperature and carefully dried under nitrogen. Subsequently, 50 µL of a 1:1 (*v:v*) mixture of trifluoroacetic anhydride (TFAA) and ethyl acetate were added, stirred for 10 s and held at room temperature for 1 h. The samples were finally thoroughly dried under nitrogen and dissolved in 50 µL of ethyl acetate containing $10^{-6}$ M methyl myristate as an internal standard. Each sample was derivatized in duplicate except for O and F blanks, which were derivatized once.

In addition, samples FGO2 (i.e., FGO with 2 days of reaction) and FGα2 were derivatized with *N, O*-bis(trimethylsilyl)trifluoroacetamide (BSTFA) and analyzed as described in Meinert *et al.*[1] to search for additional sugar-related compounds and markers indicating the formose reaction network. Briefly, 20 µL of FGO2 and FGα2 were dried under a nitrogen stream and then silylated with 10 µL BSTFA and 25 µL pyridine for 2 h at 80 °C; then cooled to room temperature and evaporated to dryness using a gentle stream of nitrogen. Finally, the derivatized samples were dissolved in 30 µL of *n*-hexane containing methyl laurate ($5 \times 10^{-5}$ M) as internal standard.

Enantioselective analysis was performed using a GC×GC Pegasus IV D instrument coupled to a time-of-flight mass spectrometer (LECO, St Joseph, Michigan, USA). The MS system operated at a storage rate of 100 Hz, with 25–400 amu mass range. The detector voltage was set to 1650 V with a solvent delay of 12 min. The temperature of the ion source and injector was set to 230 °C and the transfer line to 240 °C. A CP-Chirasil-Dex CB column (24.80 *m* × 0.25 mm, film thickness 0.25 µm, Agilent-Varian J&W, Santa Clara, California, USA) in the first dimension connected via a SilTite µ-Union connector (SGE, Restek) with a DB Wax column (1.55 m × 0.1 mm, film thickness 0.1 µm) in the second dimension were used. Modulation between the columns was provided by a two-stage thermal jet modulator using liquid nitrogen with a modulation time of 5 s. Helium was used as carrier gas at a constant flow rate of 1.2 mL $min^{-1}$. Samples were injected in splitless mode through an Agilent autosampler. The temperature of the primary column was held at 55 °C for 1 min, increased to 85 °C at a rate of 10 °C $min^{-1}$ and held for 8 min, then increased to 125 °C at a rate of 2 °C $min^{-1}$ with an isothermal hold of 8 min, further increased to 170 °C at a rate of 2 °C $min^{-1}$, and finally heated to 190 °C at a rate of 10 °C $min^{-1}$ and held for 5 min. The secondary oven used a constant temperature offset of 25 °C and the modulator temperature was set 15 °C above the secondary oven temperature. The ChromaTOF™ software from LECO Corp. was used to identify and quantify the sugar and sugar-related analytes. Identification of sugar and sugar alcohols was performed comparing retention times and mass fragmentation patterns with those of reference standards analyzed under identical conditions (Table S2,3). The integration range was manually changed during the quantification process to correct the automatic data processing when necessary. Quantification of sugars and sugar-related molecules (Table S1) was achieved through a three-point (days 2 and 7) as well as a four-point external calibration curve (day 45).

### 2.3. Microscopic electronic analysis of solid altered samples

Transmission electron microscopy (TEM) microanalyses were conducted at the CINAM laboratory on individual particles from sample FO2 using a JEOL JEM 2011 TEM fitted with a Bruker X-Flash Silicon Drift Detector 5030. The beam diameter was set to ~20 nm (200 Å) in order to reach the smallest particles. The constant beam density was ~ 63.5 pA $cm^{-2}$.

### 2.4. Computational methods

Density functional theory calculations were performed using the projector-augmented wave (PAW) approximation (Blöchl et al., 1994; Kresse and Joubert, 1999) and the Perdew–Burke–Ernzerhof (PBE) density functional theory (DFT) method (Perdew et al., 1996) as implemented in the Vienna *Ab Initio* Simulation Package (VASP, version 6.3.0) (Kresse and Furthmüller, 1996a, 1996b; Kresse and Hafner, 1993), using a *k*-point density of 20 *k*-points Å based on a convergence criterion of 1 meV $atom^{-1}$. To better describe long-range van der Waals interactions, a dispersion correction term was added using the D3 method of Grimme with zero-damping function (Grimme et al., 2011). To account for the high correlation of *p*-electrons of olivine's O atoms, Dudarev's rotationally invariant DFT+*U* approach was used, with a correction of 11.61 eV; this value was obtained by performing a self-consistent linear response approach (as introduced by Cococcioni and de Gironcoli, 2005) on the unit cell of Mg-pure olivine (obtained via the Materials Project (Jain et al., 2013), *id* mp-2895, hereby referred to as *bulk*). A Γ-centered 6 × 4 × 1 *k*-point grid was used for bulk calculations. The bulk structure was optimized by plotting the cell volume with respect to the total energy using a Birch–Murnaghan equation of state, resulting in the lattice parameters *a, b* and *c* of 4.730 Å, 5.928 Å and 10.114 Å, respectively. Periodic slab calculations were performed using a $p(2 \times 1)$ supercell of a 11 Å-thick non-polar, symmetric 84-atom (120) surface unit cell constructed from the bulk structure by cleavage along the ionic $Mg^{2+}$–$O^{2-}$ interactions while keeping the covalent bonds within the $SiO_4^{4-}$ subunit intact, using an own-developed Python algorithm based on the pymatgen Python library (Ong et al., 2013). A vacuum of at least 15 Å was added in the direction perpendicular to the surface to avoid spurious interactions between slabs in neighboring calculation cells. In all calculations involving the slab, the first Brillouin zone was explored using a Γ-centered 4 × 1 × 1 *k*-point grid. Given the defect-abundant nature of the surface, geometry-guided identification of binding sites for formaldehyde was performed through a triangulation-based process often used in materials chemistry: in this, a two-dimensional Delaunay triangulation is generated in the *ab* plane, consisting of a network of triangles where triangle vertices, edge midpoints and centers closely resemble classical *atop, bridge* and *fcc/hcp* sites on closely packed solid surfaces, respectively. This process was chosen over both a grid of equally spaced points or a random distribution given its proven success in the determination of adsorption energies on solid surfaces with little human bias (Montoya and Persson, 2017). In total, this high-throughput approach yielded 64 potential adsorption sites where formaldehyde could adsorb. Preliminary adsorptions of the formaldehyde molecule atop all identified surface sites was carried out

by placing the formaldehyde molecule facing O-down 3 Å away from the surface, and optimizing using the Broyden–Fletcher–Goldfarb–Shanno (BGFS) algorithm implemented in the Atomic Simulation Environment (ASE) (Hjorth Larsen et al., 2017) and the periodic GFN1-xTB semi-empirical algorithm developed by Grimme et al. (2017). Given their high distance from the adsorbates in the proposed reaction mechanism, slab atoms at the bottom 3 layers were kept frozen at their bare-slab optimized positions, while the topmost 2 atomic layers were allowed to relax freely. Frequency calculations of all reaction intermediates were performed to confirm their stationary nature and compute thermochemical corrections. In this case, Gibbs corrections to the potential energy were calculated including the zero-point energy (ZPE), vibrational enthalpy and entropy terms obtained by means of the Thermochemistry module implemented in ASE, at the experimental temperature of 80 °C (353 K) and a partial pressure of 1 atm for all molecular species involved. Atomic charges were calculated by approximating them to the sum of the charge density within a region surrounding the atoms and enclosed by a surface delimited by a zero-flux charge density, as depicted in the Bader or atoms-in-molecules theory (Tang et al., 2009). Adsorption Gibbs free energies of all intermediates were calculated as:

$$\Delta G = G_{*A} - G_{*} - nG_{H_2CO}$$

Where $G_{*A}$ is the Gibbs energy of the adsorption complexes of interest, $G_{*}$ is the Gibbs energy of the bare slab, $G_{H_2CO}$ is the Gibbs energy of the formaldehyde molecule in the gas phase, and $n$ is the number of formaldehyde molecules contained in the system of interest.

All computational data reported in this work, including geometrical and energy data of all simulated structures, can be accessed *via* the following ioChem-BD online dataset, DOI: 10.19061/iochem-bd-6–243.

## 3. Results and discussion

### 3.1. Olivine-catalyzed sugar formation from formaldehyde

A set of experiments was conducted where we replicated hydrothermal conditions using separate anoxic reactors (see methods) to examine the prebiotic potential of the formose reaction. These experiments differed in their composition of formaldehyde (F), glycolaldehyde (G), calcium hydroxide $Ca(OH)_2$ (α), olivine (O), as well as the duration of the reactions (as shown in Table 1). The formation of sugars and sugar-related compounds was closely monitored throughout the experiments after 2, 7 and 45 days using comprehensive gas-chromatography coupled to time-of-flight mass spectrometry (GC×GC-TOFMS). The primary focus of our study was to determine the efficacy of olivine as a catalyst for the formose reaction, even in the absence of both an initiator, such as glycolaldehyde, and a conventional base catalyst.

We found that olivine can promote the formose reaction, not only when starting from a solution of formaldehyde and glycolaldehyde (FGO, Fig. S1), but also when initiated solely from formaldehyde solutions (FO, Fig. 2). The occurrence of the reaction has been demonstrated by the detection of molecular markers. These specific compounds or intermediates that are formed during the reaction can be used to trace specific chemical pathways involved in the progression of the formose reaction (Fig. 1). One such marker is the formation of various higher-carbon sugars, including ribose and glucose, which are definitive outcomes of the formose reaction. The FO samples exhibited the presence of glycolaldehyde and dihydroxyacetone, serving as the initial reactive intermediates that enable the rest of the formose reaction cascade. The identification of various configurational isomers of C3 to C6 sugar and sugar alcohols provided further evidence supporting the catalytic activity of olivine (Fig. 2, Table S1). Additionally, a qualitative examination of sugar acids and other relevant formose reaction products, such as the abundant Cannizzaro products 2-hydroxymethylglycerol (HMG) and 2-hydroxymethyltetritol (HMT) (Shigemasa et al., 1977), confirmed the intricate chemical network typically associated with the formose reaction (Table S2).

In the absence of olivine, solutions containing formaldehyde and glycolaldehyde (FG) were found to be much less efficient in generating higher sugars. Within a 2-day reaction period, the FG2 sample was limited to sugars with a maximum of 4 carbon atoms and minor amounts of arabinose -a C5 sugar (Table S1). Even with an extended reaction time of 45 days, the chemical reaction in the FG samples was ineffective to yield significant amount of higher sugar and sugar-related molecules, including those with five or six carbon atoms (Fig. 3). Control experiments of formaldehyde (F) and olivine (O) in separate reactors supported the conclusion that olivine exhibited catalytic activity towards

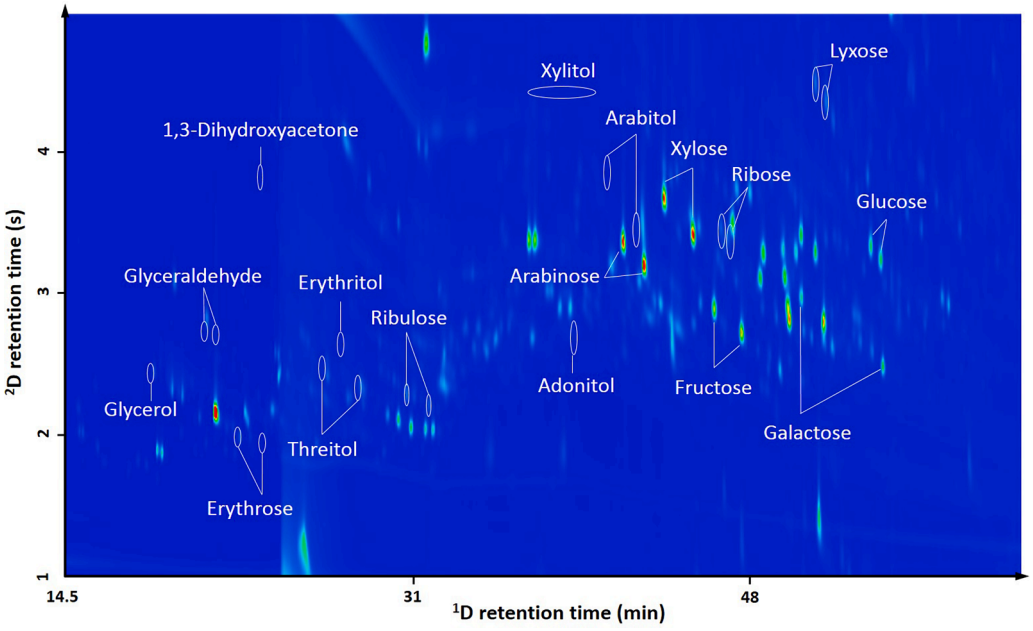


**Fig. 2.** Olivine-catalyzed sugar formation in a hydrothermally altered formaldehyde solution. Two-dimensional gas chromatogram of the sugar products after 2 days of hydrothermal alteration of formaldehyde in the presence of olivine (FO2). The sugars are resolved on a Chirasil-Dex column in the first dimension ($^1$D) coupled to a DB Wax in the second dimension ($^2$D) as MBA-TFA derivatives (see Methods). Mass-to-charge ratios *m/z* 84, 85, 97, 113, and 127 are displayed.

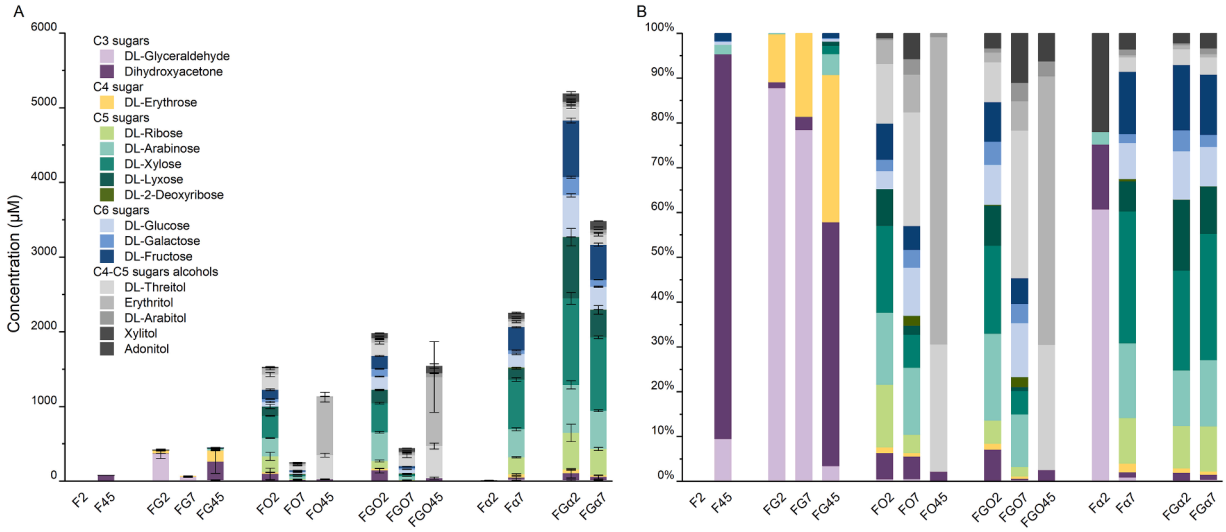


**Fig. 3.** Sugar evolution depending on initial composition and hydrothermal alteration time. A, The molar concentrations of sugars and sugar alcohols were determined in samples after 2, 7, and 45 days of aqueous alteration at an initial temperature of 80 °C. Various combinations containing formaldehyde (F), glycolaldehyde (G), Olivine (O), or $Ca(OH)_2$ (α) were investigated. Uncertainties were determined by calculating the standard deviation (± 1 s) of the average value from two replicate derivatizations, each injected twice ($n = 4$), unless otherwise specified. For detailed information on concentrations, please refer to Table S2. B, Total sugar content per sample normalized to 100 %, allowing for a clearer observation of the evolution of sugars based on their respective classes.

formaldehyde due to the absence or very low abundances of higher-carbon sugars in these samples (Fig. 3). Due to the detection of glycerol in the olivine sample (O) and the potential for contamination during the experiments, the evolution of glycerol content in the different samples, as reported in Table S1, is not depicted in Fig. 3.

### 3.2. Comparing the catalytic sugar production with olivine vs calcium hydroxide

We compared our findings using olivine as a catalyst with hydrothermal alteration experiments that employed the traditional $Ca(OH)_2$ catalyst (α) for the formose reaction. In general, we identified various sugar and sugar-related molecules ranging from 3 to 6 carbon atoms in both sets of samples, indicating comparable molecular diversity (Figs. 3 and S2). However, when it came to the quantitative production of sugars, the mixtures containing formaldehyde and glycolaldehyde in the presence of calcium hydroxide (FGα) were more efficient compared to the same initial reagents in the presence of olivine (FGO). On the other hand, the overall sugar production in the olivine-catalyzed solution of formaldehyde only (FO2) proceeded at a faster rate than in the calcium hydroxide-catalyzed formaldehyde solution (Fα2). The initiation of formaldehyde by olivine in the absence of glycolaldehyde was highly efficient after just 2 days (FO2), whereas the production of larger sugar species with calcium hydroxide occurred only after longer reaction times (Fα7).

Due to the favorable conditions of the formose reaction in slightly alkaline environments (Kopetzki and Antonietti, 2011), $Ca(OH)_2$, serves as both a catalyst and a pH "buffer" of the formose reaction. Achieving alkaline conditions is also possible through the use of olivine. In our experimental system, olivine dissolution was observed due to the small grain size (<10 μm) and moderate temperature conditions (Oelkers et al., 2018). Microscopic analysis after 2 days of reaction revealed the presence of phyllosilicates in proximity to the original olivine grains (Fig. S3), indicating a serpentinization process that transforms the olivine. This dissolution process acts as a buffer by consuming $H^+$ during silicate dissolution and releasing ions such as $Mg^{2+}$ and $Fe^{2+}$ (Oelkers et al., 2018). A possible dissolution reaction for olivine can be (if the reaction is total, which is never the case) : $2\,Mg_{1.8}Fe_{0.2}SiO_4 + 3H_2O \rightarrow [2\,(Mg^{2+})_{1.8} + 2\,(Fe^{2+})_{0.2} + 2\,SiO_4^{4-} + 3H_2O] \rightarrow (Mg_{2.6},Fe_{0.4})Si_2O_5(OH)_4$ (serpentine) + $Mg(OH)_2$ (brucite). After the completion of the reactions, the pH of FO and FGO samples was still close to neutral pH, while the pH of the F and FG samples, which lacked olivine, measured between 4 and 5. For the FGα sample, initially possessing a pH of 10 due to calcium hydroxide, the pH dropped to 5–6 after 2 and 7 days. The presence of olivine, which maintains a neutral to slightly alkaline pH, thus promotes the production of sugars up to C6 after 2 days of reaction. In contrast, in the absence of olivine under more acidic conditions, only C3 and C4 sugars are formed in the FG samples. However, the role of olivine extends beyond pH regulation, as the $Mg^{2+}$and $Fe^{2+}$ cations released from its dissolution likely function as chelators for enediolate intermediates, similar to the demonstrated role of $Ca^{2+}$ in previous studies (Gabel and Ponnamperuma, 1967; Mizuno and Weiss, 1974). In our conditions, the phyllosilicates formed can also facilitate aldol reactions by interacting with glyceraldehyde or aldohexoses/pentose through van der Waals forces at their surface (Kleber et al., 2015).

### 3.3. Sugar diversity and their evolution over time

In addition to the sugars/sugar alcohols and sugar acids reported in Table S1 and Table S2, respectively, numerous other sugar compounds and related molecules were detected in the hydrothermally altered samples. However, the complex nature of these mixtures posed challenges in the chromatographic analyses and their identification, thereby limiting the number of monitored formose products, in addition to the lack of standards. Nevertheless, the variety of compounds identified in this study exhibited significant heterogeneity. These compounds comprised not only aldoses but also other relevant sugar-related compounds like alcohols and hydroxycarboxylic acids that are essential of contemporary metabolism (Omran et al., 2020).

The formose reaction is known to exhibit regioselectivity, which refers to the preferential formation of specific regioisomers during the reaction (Delidovich et al., 2014; Robinson et al., 2022). Our study suggests a regioselectivity among the C5 sugars favoring xylose and arabinose over lyxose and ribose in both calcium hydroxide and olivine-catalyzed reactions. However, further studies are required to validate this trend.

After 2 days of hydrothermal alteration, a decrease in both the diversity and quantity of sugars, primarily -oses, was observed across all samples, except for Fα, despite no significant change in pH of the catalyzed samples (Table 1). Upon alteration times of 45 days, the identified

molecules remaining in the samples containing olivine (FO45, FGO45) predominantly comprised C4 sugar alcohols (Fig. 3B), generated in significant amounts through the Cannizzaro reaction (Fig. 1). Previous research has indicated that even minute quantities of naturally occurring carbohydrates (in the parts per million range) can serve as sufficient catalysts for initiating the formose reaction (Delidovich et al., 2014; Socha et al., 1980). However, our experiments employing only formaldehyde (F2 and F45) demonstrated that the amount of glycolaldehyde produced under such conditions was insufficient to effectively trigger the formation of higher sugar molecules. Instead, the Cannizzaro reaction operated as an alternative pathway. Even when glycolaldehyde was added to formaldehyde, the predominant products were C3 sugars in the absence of any catalyst, even with prolonged reaction times (FG2–FG45).

### 3.4. Mechanistic insights into formaldehyde activation on olivine surfaces

Based on our experimental results, we employed quantum chemical simulations to gain detailed atomistic insights into the processes studied, with a specific focus on the initiation of the formose reaction involving the condensation of two formaldehyde molecules. The olivine surface was modelled using a (120) crystalline slab model (Fig. 4a), derived from Mg-pure olivine (i.e., forsterite, $Mg_2SiO_4$). This surface termination is theoretically predominant in olivine nanoparticles (Bruno et al., 2014) and exhibits a nearly uniform distribution of potentially active Lewis acidic ($Mg^{2+}$) and basic ($O^{2-}$) surface sites, which have been demonstrated to be crucial in the Mg-silicate-catalyzed ethanol condensation step in the Lebedev process (Chung et al., 2023) .

We first assessed the adsorption of formaldehyde on 64 representative surface sites (Fig. S4a) obtained through triangulation (see Methods). The proximity of surface $Mg^{2+}$ and $O^{2-}$sites promotes the adsorption of formaldehyde, where the oxygen atom of formaldehyde binds to a $Mg^{2+}$ site, and the carbon atom interacts with an $O^{2-}$ site, resulting in an activated carbonyl species with enhanced reactivity. Potential competitivity with water towards adsorption on the selected active site was assessed by replacing the formaldehyde species with a single water molecule occupying the same $Mg^{2+}$ binding site (as depicted in Fig. S5). This reveals water and formaldehyde adsorption to be almost equally favored on the surface at the experimental conditions, as they display similar potential binding energies of −32.05 and −31.13 kcal $mol^{-1}$, respectively. indicating a likely coexistence between formaldehyde and water on the surface. Subsequently, we investigated the capacity of the basic surface $O^{2-}$ sites to dehydrogenate the activated formaldehyde. For this purpose, we selected a specific adsorbed formaldehyde molecule positioned near an $O^{2-}$ surface site (I1, Fig. 4b) with one of the most favorable adsorption energies (−14.14 kcal $mol^{-1}$, Fig. 4c). Our calculations show that the surface $O^{2-}$ can exergonically abstract a hydrogen atom from formaldehyde, yielding a carbonyl-ene-like species interacting with two surface $Mg^{2+}$ sites via the oxygen and carbon atoms (I2, Fig. 4b). The energetic analysis of this

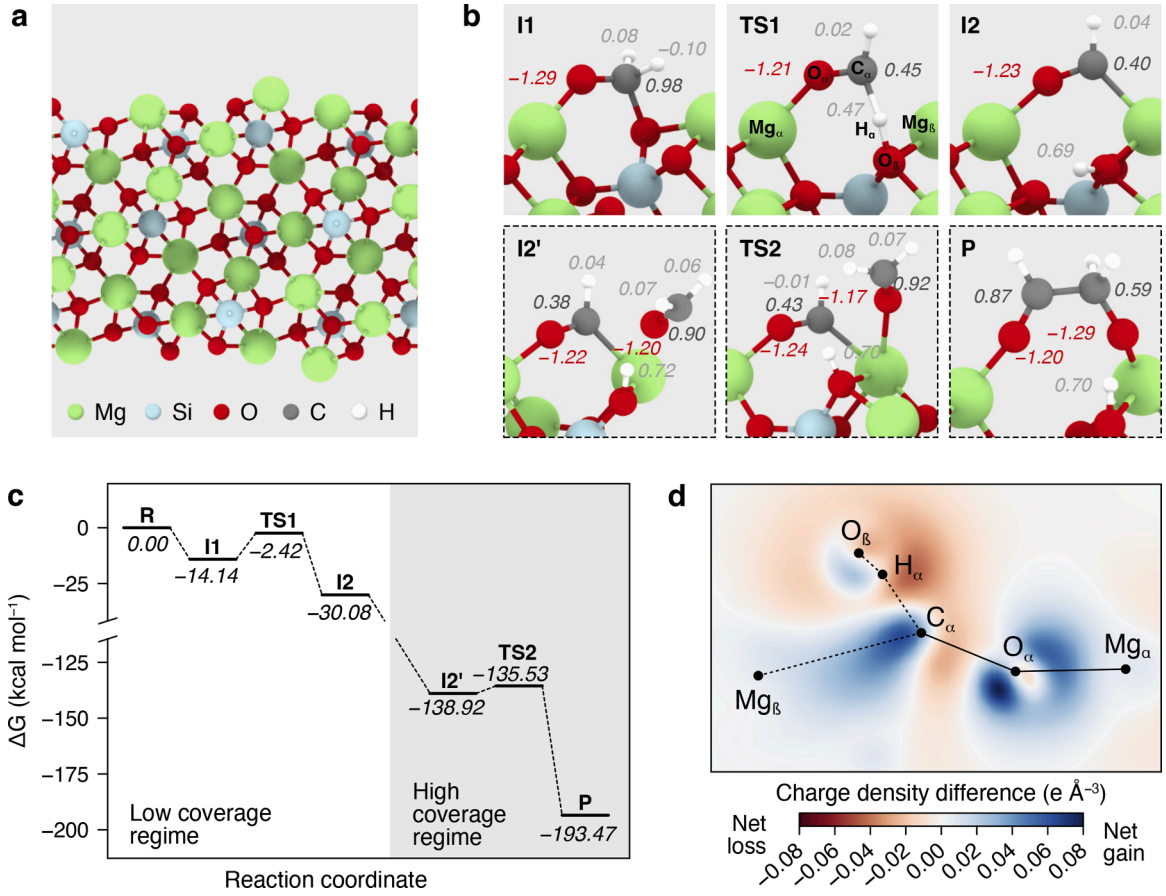


**Fig. 4.** Exploring the catalytic potential of olivine surfaces through computational insights. a, Side view of the unit cell of the Mg-rich olivine surface model used for simulations. b, Representations of the stationary points identified in the proposed mechanism, namely, in the activation and deprotonation of formaldehyde on the surface in a low coverage regime (I1, TS1 and I2) and in the condensation of formaldehyde within a high coverage regime (I2', TS2 and P). Relevant atomic charges are represented in italics beside each atom in their respective color. c, Calculated free energy profile (in kcal $mol^{-1}$ and $T = 353$ K) of the proposed reaction pathway for the formation of glycolaldehyde. Labels of the species are referenced to those in panel b. d, Top view of the cumulative charge density difference between the adsorbed species and the surface of TS1. A net gain and loss in charge density is denoted in blue and red, respectively. Relevant atoms are denoted as dots in the *ab* plane.

deprotonation process reveals the presence of a transition state (TS1, Fig. 4b) with an intrinsic Gibbs energy activation barrier of 11.72 kcal $mol^{-1}$, which can be overcome under our experimental conditions (80 °C). Notably, the presence of an activated carbonyl-ene species has been shown to be crucial for the reactivity with formaldehyde, leading to the formation of glycolaldehyde in the gas phase (Eckhardt et al., 2018). To explore this further, we simulated the reaction between the deprotonated formaldehyde with a physisorbed (non-deprotonated) formaldehyde molecule on the surface. In this scenario, we considered a high coverage regime where all the adsorption sites surrounding the deprotonated formaldehyde are saturated by other adsorbed formaldehyde species (as depicted in Fig. S4b) which is more consistent with the experimental conditions compared to a low coverage regime. Within this model, a subsequent formaldehyde molecule can be exergonically stabilized atop the ligand phase (I2', Fig. 4b), enabling it to react with the deprotonated formaldehyde and yielding glycolaldehyde in a highly exergonic process through a transition state (TS2, Fig. 4b) with an intrinsic Gibbs energy barrier of 3.39 kcal $mol^{-1}$ (Fig. 4c).

The catalytic activity of the surface in activating and deprotonating formaldehyde was assessed by analyzing the charge density difference between the adsorbates and the surface in TS1 (Fig. 4d). This revealed a decrease in charge density in the $C_\alpha$–$H_\alpha$ bond of formaldehyde upon the transfer of $H_\alpha$ to $O_\beta$ (red area between $C_\alpha$ and $H_\alpha$). This is followed by an increase in charge density between $C_\alpha$ of formaldehyde and the nearest surface $Mg^{2+}$ atom (blue area between $C_\alpha$ and $Mg_\beta$). Thus, the surface induces a polarity inversion on the deprotonated formaldehyde, which promotes the umpolung mechanism necessary for the condensation of formaldehyde towards glycolaldehyde. This demonstrates the necessity of surface sites with enhanced acidity and basicity in promoting the activation of formaldehyde, rendering Earth- and space-abundant silicates exceptional initiators and catalysts for the formose reaction.

## 4. Concluding remarks and broader application of silicates in prebiotic systems

This research demonstrates the significant role that abundant minerals found on planetary surfaces, specifically olivine silicates, may have played in the chemical reactions involved in the evolution of prebiotic systems in early Earth' aqueous environments. The presence of olivine allowed the formose reaction, leading to the formation of sugars and a wide range of sugar-related molecules typically linked with the occurrence of a formose network. While the catalytic effect of olivine on the auto-catalytic cycle is likely due to its ability to stabilize enediol forms with $Mg^{2+}$ (Gabel and Ponnamperuma, 1967; Mizuno and Weiss, 1974), the mechanism behind the initiation step has remained unknown. Our study highlights that olivine (Mg-rich) can initiate the reaction, only from formaldehyde, an initiation step usually achieved via the addition of other carbohydrates, or the use of photochemistry (ultra-violet irradiation). Our theoretical work provided insight into a plausible mechanism whereby the olivine surface deprotonates formaldehyde and enables its dimerization. This mineral surface-assisted mechanism represents a non-radical pathway that overcomes the unfavorable initiation step of the formose reaction, as confirmed experimentally and through quantum mechanical calculations. The olivine dissolution also maintained the solution at an elevated pH compared to solutions lacking olivine, which promoted further progression of the reaction. As demonstrated here, neither glycolaldehyde nor calcium hydroxide alone proved as effective in initiating, catalyzing, and buffering the entire formose reaction as olivine.

Furthermore, despite the formose reaction being generally considered non-selective, it has been observed that the reaction can exhibit different self-organization patterns depending on the environmental conditions (Robinson et al., 2022). For instance, previous research demonstrated that certain chemical pathways of the formose reaction can be influenced to yield specific product compositions through a driving force (Robinson et al., 2022; Surman et al., 2019). Expanding on this concept, we propose that minerals like olivine, present in diverse environmental settings, could potentially guide the formose reaction towards the preferential formation of individual sugars, as indicated by the varying yields of sugars with the same number of carbon atoms observed in our study. However, this hypothesis requires additional dedicated investigations with other mineral composition, may be enriched in iron (Peters et al., 2023) and conducting comprehensive analyses of the reaction products. Additionally, our experiments highlight the challenge of maintaining sugar stability in aqueous environments. To address this concern in prebiotic scenarios, sugars can be rapidly utilized in subsequent chemical reactions, stabilized through interactions with other molecules (Kim et al., 2011), or continuously regenerated in volcanic settings through the interaction of formaldehyde and olivine, as demonstrated in our study.

The discovery of the influence of mineral activity on a well-known chemical reaction such as the formose reaction, which holds significant importance in prebiotic contexts, represents a notable advancement in our understanding of how abiotic reactions can be influenced by the surrounding mineral environment (Rimola et al., 2019; Vinogradoff et al., 2020). Indeed, the mineral can activate specific molecules and allow them for further chemical reaction without other energy source (such as photochemistry). The formose reaction's role in establishing an autocatalytic system for prebiotic chemistry, in addition to its contribution to sugar formation, positions minerals as crucial components of prebiotic environments. By applying similar approaches to other reaction networks that are relevant to prebiotic conditions (Miller, 1957), we can gain new insights into the synthesis of life's fundamental building blocks and the development of dynamic chemical networks in specific environments (Danger et al., 2022).

Supplementary files

The supplementary files include tables of sugar identification and quantifications for all samples, additional figures of hydrothermally-altered samples using multidimensional gas-chromatography coupled to time-of-flight mass-spectrometry analyses; the characterization of hydrothermally-altered samples by TEM and additional representations of the surface models used in simulations are shown.

## CRediT authorship contribution statement

**Vassilissa Vinogradoff:** Conceptualization, Investigation, Writing – original draft, Writing – review & editing, Formal analysis, Supervision. **Vanessa Leyva:** Formal analysis, Writing – review & editing. **Eric Mates-Torres:** Methodology, Writing – original draft, Writing – review & editing. **Raphael Pepino:** Formal analysis, Writing – review & editing. **Grégoire Danger:** Writing – review & editing. **Albert Rimola:** Methodology, Writing – original draft, Writing – review & editing. **Lauryane Cazals:** Investigation, Formal analysis. **Coline Serra:** Investigation, Writing – review & editing. **Robert Pascal:** Writing – review & editing. **Cornelia Meinert:** Formal analysis, Supervision, Writing – original draft, Writing – review & editing.

## Declaration of competing interest

The authors declare that they have no known competing financial interests or personal relationships that could have appeared to influence the work reported in this paper.

## Acknowledgements

We gratefully acknowledge support from the CNRS INSU (AAP 2023 FORMOLIFE project). This work was funded by the European Research Council under the European Union's Horizon 2020 research and innovation program under grant agreement 804144 (ERC-ALIFE, C.M.) and grant agreement 865657 (ERC-QUANTUMGRAIN, A.R.). MICINN (project PID2021-126427NB-I00) is also acknowledged. V.V. thanks Olivier Grauby (CINAM, Aix-Marseille University) for TEM

measurements. E.M.-T. thankfully acknowledges financial support by the Spanish Ministry of Universities and the European Union's Next Generation EU fund. We also thankfully acknowledge the computer resources and assistance provided by the Barcelona Supercomputing Center and CSUC.

## Supplementary materials

Supplementary material associated with this article can be found, in the online version, at doi:10.1016/j.epsl.2023.118558.

## References


Blöchl, P.E., Jepsen, O., Andersen, O.K., 1994. Improved tetrahedron method for Brillouin-zone integrations. Phys. Rev. B 49, 16223–16233. https://doi.org/10.1103/PhysRevB.49.16223.

Breslow, R., 1959. On the mechanism of the formose reaction. Tetrahedron Lett 1, 22–26. https://doi.org/10.1016/S0040-4039(01)99487-0.

Bruno, M., Massaro, F.R., Prencipe, M., Demichelis, R., De La Pierre, M., Nestola, F., 2014. Ab initio calculations of the main crystal surfaces of forsterite (Mg2SiO4): a preliminary study to understand the nature of geochemical processes at the olivine interface. J. Phys. Chem. C 118, 2498–2506. https://doi.org/10.1021/jp409837d.

Butlerov, A.M., 1861. Formation synthétique d'une substance sucrée. CR Acad. Sci. 53, 145–147.

Cairns-Smith, A.G., Ingram, P., Walker, G.L., 1972. Formose production by minerals: possible relevance to the origin of life. J. Theor. Biol. 35, 601–604. https://doi.org/10.1016/0022-5193(72)90153-1.

Chung, S.H., Li, T., Shoinkhorova, T., Komaty, S., Ramirez, A., Mukhambetov, I., Abou-Hamad, E., Shterk, G., Telalovic, S., Dikhtiarenko, A., Sirks, B., Lavrik, P., Tang, X., Weckhuysen, B.M., Bruijnicx, P.C.A., Gascon, J., Ruiz-Martínez, J., 2023. Origin of active sites on silica–magnesia catalysts and control of reactive environment in the one-step ethanol-to-butadiene process. Nat. Catal. 6, 363–376. https://doi.org/10.1038/s41929-023-00945-0.

Cleaves, H.J., 2008. The prebiotic geochemistry of formaldehyde. Precambrian Res 164, 111–118. https://doi.org/10.1016/j.precamres.2008.04.002.

Cococcioni, M., de Gironcoli, S., 2005. Linear response approach to the calculation of the effective interaction parameters in the $\mathrm{LDA}+\mathrm{U}$ method. Phys. Rev. B 71, 035105. https://doi.org/10.1103/PhysRevB.71.035105.

Cooper, G., Kimmich, N., Belisle, W., Sarinana, J., Brabham, K., Garrel, L., 2001. Carbonaceous meteorites as a source of sugar-related organic compounds for the early Earth. Nature 414, 879–883. https://doi.org/10.1038/414879a.

Danger, G., Le Sergeant d'Hendecourt, L., Vinogradoff, V., Pascal, R., 2022. New directions for an experimental approach to the chemistry of the origin of life. Prebiotic Chemistry and Life's Origin. Royal Society of Chemistry.

Delidovich, I.V., Simonov, A.N., Taran, O.P., Parmon, V.N., 2014. Catalytic formation of monosaccharides: from the formose reaction towards selective synthesis. ChemSusChem 7, 1833–1846. https://doi.org/10.1002/cssc.201400040.

Eckhardt, A.K., Linden, M.M., Wende, R.C., Bernhardt, B., Schreiner, P.R., 2018. Gas-phase sugar formation using hydroxymethylene as the reactive formaldehyde isomer. Nat. Chem. 10, 1141–1147. https://doi.org/10.1038/s41557-018-0128-2.

Furukawa, Y., Chikaraishi, Y., Ohkouchi, N., Ogawa, N.O., Glavin, D.P., Dworkin, J.P., Abe, C., Nakamura, T., 2019. Extraterrestrial ribose and other sugars in primitive meteorites. Proc. Natl. Acad. Sci 116, 24440–24445. https://doi.org/10.1073/pnas.1907169116.

Gabel, N.W., Ponnamperuma, C., 1967. Model for origin of monosaccharides. Nature 216, 453.

Grimme, S., Bannwarth, C., Shushkov, P., 2017. A robust and accurate tight-binding quantum chemical method for structures, vibrational frequencies, and noncovalent interactions of large molecular systems parametrized for all spd-block elements (Z = 1–86). J. Chem. Theory Comput. 13, 1989–2009. https://doi.org/10.1021/acs.jctc.7b00118.

Grimme, S., Ehrlich, S., Goerigk, L., 2011. Effect of the damping function in dispersion corrected density functional theory. J. Comput. Chem. 32, 1456–1465. https://doi.org/10.1002/jcc.21759.

Haas, M., Lamour, S., Christ, S.B., Trapp, O., 2020. Mineral-mediated carbohydrate synthesis by mechanical forces in a primordial geochemical setting. Commun. Chem. 3, 1–6. https://doi.org/10.1038/s42004-020-00387-w.

Hjorth Larsen, A., Jørgen Mortensen, J., Blomqvist, J., Castelli, I.E., Christensen, R., Dułak, M., Friis, J., Groves, M.N., Hammer, B., Hargus, C., Hermes, E.D., Jennings, P.C., Bjerre Jensen, P., Kermode, J., Kitchin, J.R., Leonhard Kolsbjerg, E., Kubal, J., Kaasbjerg, K., Lysgaard, S., Bergmann Maronsson, J., Maxson, T., Olsen, T., Pastewka, L., Peterson, A., Rostgaard, C., Schiøtz, J., Schütt, O., Strange, M., Thygesen, K.S., Vegge, T., Vilhelmsen, L., Walter, M., Zeng, Z., Jacobsen, K.W., 2017. The atomic simulation environment-a Python library for working with atoms. J. Phys. Condens. Matter Inst. Phys. J. 29, 273002 https://doi.org/10.1088/1361-648X/aa680e.

Jain, A., Ong, S.P., Hautier, G., Chen, W., Richards, W.D., Dacek, S., Cholia, S., Gunter, D., Skinner, D., Ceder, G., Persson, K.A., 2013. Commentary: the materials project: a materials genome approach to accelerating materials innovation. APL Mater. 1, 011002 https://doi.org/10.1063/1.4812323.

Kim, H.J., Ricardo, A., Illangkoon, H.I., Kim, M.J., Carrigan, M.A., Frye, F., Benner, S.A., 2011. Synthesis of carbohydrates in mineral-guided prebiotic cycles. J. Am. Chem. Soc. 133, 9457–9468. https://doi.org/10.1021/ja201769f.

Kleber, M., Eusterhues, K., Keiluweit, M., Mikutta, C., Mikutta, R., Nico, P.S., 2015. Chapter one - mineral–organic associations: formation, properties, and relevance in soil environments. Ed.. In: Sparks, D.L. (Ed.), Advances in Agronomy. Academic Press, pp. 1–140. https://doi.org/10.1016/bs.agron.2014.10.005.

Kopetzki, D., Antonietti, M., 2011. Hydrothermal formose reaction. New J. Chem. 35, 1787–1794. https://doi.org/10.1039/C1NJ20191C.

Kresse, G., Furthmüller, J., 1996a. Efficiency of ab-initio total energy calculations for metals and semiconductors using a plane-wave basis set. Comput. Mater. Sci. 6, 15–50. https://doi.org/10.1016/0927-0256(96)00008-0.

Kresse, G., Furthmüller, J., 1996b. Efficient iterative schemes for ab initio total-energy calculations using a plane-wave basis set. Phys. Rev. B 54, 11169–11186. https://doi.org/10.1103/PhysRevB.54.11169.

Kresse, G., Hafner, J., 1993. Ab initio molecular dynamics for liquid metals. Phys. Rev. B 47, 558–561. https://doi.org/10.1103/PhysRevB.47.558.

Kresse, G., Joubert, D., 1999. From ultrasoft pseudopotentials to the projector augmented-wave method. Phys. Rev. B 59, 1758–1775. https://doi.org/10.1103/PhysRevB.59.1758.

Lambert, J.B., Gurusamy-Thangavelu, S.A., Ma, K., 2010. The silicate-mediated formose reaction: bottom-up synthesis of sugar silicates. Science 327, 984–986. https://doi.org/10.1126/science.1182669.

Larralde, R., Robertson, M.P., Miller, S.L., 1995. Rates of decomposition of ribose and other sugars: implications for chemical evolution. Proc. Natl. Acad. Sci 92, 8158–8160. https://doi.org/10.1073/pnas.92.18.8158.

Meinert, C., Myrgorodska, I., Marcellus, P.de, Buhse, T., Nahon, L., Hoffmann, S.V., d'Hendecourt, L.L.S., Meierhenrich, U.J., 2016. Ribose and related sugars from ultraviolet irradiation of interstellar ice analogs. Science 352, 208–212.

Miller, S.L., 1957. The mechanism of synthesis of amino acids by electric discharges. Biochim. Biophys. Acta 23, 480–489. https://doi.org/10.1016/0006-3002(57)90366-9.

Miyazaki, Y., Korenaga, J., 2022. A wet heterogeneous mantle creates a habitable world in the Hadean. Nature 603, 86–90. https://doi.org/10.1038/s41586-021-04371-9.

Mizuno, T., Weiss, A.H., 1974. Synthesis and utilization of formose sugars. Eds.. In: Tipson, R.S., Horton, D. (Eds.), Advances in Carbohydrate Chemistry and Biochemistry. Academic Press, pp. 173–227. https://doi.org/10.1016/S0065-2318(08)60250-4.

Montoya, J.H., Persson, K.A., 2017. A high-throughput framework for determining adsorption energies on solid surfaces. Npj Comput. Mater. 3, 1–4. https://doi.org/10.1038/s41524-017-0017-z.

Oelkers, E.H., Declercq, J., Saldi, G.D., Gislason, S.R., Schott, J., 2018. Olivine dissolution rates: a critical review. Chem. Geol. 500, 1–19. https://doi.org/10.1016/j.chemgeo.2018.10.008.

Omran, A., Menor-Salvan, C., Springsteen, G., Pasek, M., 2020. The messy alkaline formose reaction and its link to metabolism. Life 10, 125. https://doi.org/10.3390/life10080125.

Ong, S.P., Richards, W.D., Jain, A., Hautier, G., Kocher, M., Cholia, S., Gunter, D., Chevrier, V.L., Persson, K.A., Ceder, G., 2013. Python Materials Genomics (pymatgen): a robust, open-source python library for materials analysis. Comput. Mater. Sci. 68, 314–319. https://doi.org/10.1016/j.commatsci.2012.10.028.

Perdew, J.P., Burke, K., Ernzerhof, M., 1996. Generalized gradient approximation made simple. Phys. Rev. Lett. 77, 3865–3868. https://doi.org/10.1103/PhysRevLett.77.3865.

Peters, S., Semenov, D.A., Hochleitner, R., Trapp, O., 2023. Synthesis of prebiotic organics from CO2 by catalysis with meteoritic and volcanic particles. Sci. Rep. 13, 6843. https://doi.org/10.1038/s41598-023-33741-8.

Rimola, A., Sodupe, M., Ugliengo, P., 2019. Role of mineral surfaces in prebiotic chemical evolution. In Silico Quantum Mech. Stud. Life 9, 10. https://doi.org/10.3390/life9010010.

Ritson, D., Sutherland, J.D., 2012. Prebiotic synthesis of simple sugars by photoredox systems chemistry. Nat. Chem. 4, 895–899. https://doi.org/10.1038/nchem.1467.

Robinson, W.E., Daines, E., van Duppen, P., de Jong, T., Huck, W.T.S., 2022. Environmental conditions drive self-organization of reaction pathways in a prebiotic reaction network. Nat. Chem. 14, 623–631. https://doi.org/10.1038/s41557-022-00956-7.

Russell, M.J., Ponce, A., 2020. Six 'must-have' minerals for life's emergence: olivine, pyrrhotite, bridgmanite, serpentine, fougerite and mackinawite. Life 10, 291. https://doi.org/10.3390/life10110291.

Schwartz, A.W., de Graaf, R.M., 1993. The prebiotic synthesis of carbohydrates: a reassessment. J. Mol. Evol. 36, 101–106. https://doi.org/10.1007/BF00166245.

Shigemasa, Y., Matsuda, Y., Sakazawa, C., Matsuura, T., 1977. Formose reactions. II. The photochemical formose reaction. Bull. Chem. Soc. Jpn. 50, 222–226. https://doi.org/10.1246/bcsj.50.222.

Socha, R.F., Weiss, A.H., Sakharov, M.M., 1980. Autocatalysis in the formose reaction. React. Kinet. Catal. Lett. 14, 119–128. https://doi.org/10.1007/BF02061275.

Surman, A.J., Rodriguez-Garcia, M., Abul-Haija, Y.M., Cooper, G.J.T., Gromski, P.S., Turk-MacLeod, R., Mullin, M., Mathis, C., Walker, S.I., Cronin, L., 2019. Environmental control programs the emergence of distinct functional ensembles from unconstrained chemical reactions. Proc. Natl. Acad. Sci 116, 5387–5392. https://doi.org/10.1073/pnas.1813987116.

Tang, W., Sanville, E., Henkelman, G., 2009. A grid-based Bader analysis algorithm without lattice bias. J. Phys. Condens. Matter 21, 084204. https://doi.org/10.1088/0953-8984/21/8/084204.

Vinogradoff, V., Le Guillou, C., Bernard, S., Viennet, J.C., Jaber, M., Remusat, L., 2020. Influence of phyllosilicates on the hydrothermal alteration of organic matter in asteroids: experimental perspectives. Geochim. Cosmochim. Acta 269, 150–166. https://doi.org/10.1016/j.gca.2019.10.029.